$(p,2p)$ and (p,pd) reactions on ^{3}H at 45.6 MeV†

D. I. Bonbright, S. A. Elbakr,* A. Houdayer,‡ C. A. Miller,§ D. J. Roberts, E. S. Y. Tin,‖ W. T. H. van Oers, and J. W. Watson

Cyclotron Laboratory, Department of Physics, University of Manitoba, Winnipeg, Canada R3T 2N2

(Received 14 July 1975)

The reactions ^{3}H$(p,2p)nn$, ^{3}H$(p,pd)n$, and ^{3}He$(p,2p)d$, ^{3}He$(p,2p)pn$, and ^{3}He$(p,pd)p$ have been studied at 45.6 and 45.0 MeV, respectively, using coplanar symmetric and asymmetric geometries. An angular correlation has been obtained for the ^{3}He$(p,2p)[nn]$ reaction, where $[nn]$ denotes an n-n pair with low energy for its relative motion. Energy sharing data for this reaction have also been obtained at a number of coplanar asymmetric angle pairs which allow zero spectator momentum. Within the framework of the plane wave impulse approximation the extracted momentum distributions of the $p+[nn]$ system in ^{3}H and the $p+d$ and $p+d^*$ systems in ^{3}He are compared with predictions calculated using relatively simple wave functions for ^{3}H, ^{3}He, d, d^*, and $[nn]$. Reasonable agreement between the shapes of the extracted and theoretical momentum distributions has been obtained, but there exist differences between the momentum distributions extracted from the angular correlation and energy sharing data. The ^{3}H(p,pd) quasifree scattering enhancements exhibit shifts in the peak position away from the minimum in the momentum of the spectator neutron. Comparison of the four-body continua of the ^{3}H$(p,2p)nn$ reactions reveals enhancements which can be interpreted as due to pseudo-two-body processes, namely, the p-d^* quasifree scattering process and the reaction $p+{}^3\mathrm{H} \rightarrow d^*+d^*$.

[NUCLEAR REACTIONS ^{3}H$(p,2p)$, ^{3}H(p,pd), $T_1=45.6$ MeV; ^{3}He$(p,2p)$, ^{3}He$(p,2p)$, $T_1=45.0$ MeV; measured $d\sigma/(dT_3 d\Omega_3 d\Omega_4)$ in coplanar geometry; deduced momentum distributions using PWIA; compared with theoretical momentum distributions; investigated four-body continua.]

I. INTRODUCTION

In recent years extensive studies[1-7] have been made of the $(p,2p)$ and (p,pd) reactions on ^{3}He at incident energies between 35 and 590 MeV with the aim of extracting nuclear structure information. In most cases, kinematical conditions favoring p-p and p-d quasifree scattering were chosen.

Because of the inherent difficulty in handling radioactive tritium, few coincidence measurements have been made of proton induced breakup of ^{3}H.[8] Until now the only existing $(p,2p)$ data were those of Fritts *et al.* who investigated the ^{3}H$(p,2p)$-nn and ^{3}He$(p,2p)pn$ reactions at 20 MeV. The purpose of their experiment was to obtain information about the unknown neutron-neutron scattering parameters using a comparison procedure with a reaction characterized by a final-state interaction which can be expressed in terms of known nucleon-nucleon scattering parameters. In the present work, the ^{3}H$(p,2p)nn$ and ^{3}H$(p,pd)n$ reactions have been studied at 45.6 MeV with the objective of determining the interference of various contributing reaction mechanisms with the dominant quasifree scattering process. In addition, investigation of the ^{3}H$(p,2p)nn$ reaction might yield information on the possible existence of excited states of the three-nucleon system. In two-body breakup of ^{3}H and ^{3}He, such excited states are restricted to be $T=\frac{1}{2}$, whereas in three-body breakup of the target both $T=\frac{1}{2}$ and $T=\frac{3}{2}$ excited states are allowed. In particular, the presence of an excited state in ^{3}H will manifest itself in the continuum as an enhancement parallel to one or both of the energy axes.[9] To complement earlier studies, some additional measurements were made of the ^{3}He$(p,2p)d$ and ^{3}He$(p,2p)pn$ reactions at 45.0 MeV.

The data obtained in $(p,2p)$ and (p,pd) quasifree scattering studies are usually analyzed using the plane wave (PWIA) or distorted wave impulse approximations (DWIA). In the PWIA it is assumed that the incident particle interacts directly with only one of the constituent particles while the remainder of the nucleus behaves as a spectator. For a reaction of the type 2(1, 34)5, the PWIA leads to the well-known expression:

$$\frac{d\sigma}{dT_3 d\Omega_3 d\Omega_4} = F\left(\frac{d\sigma}{d\Omega}\right)^{1-4'} N|\Phi(\vec{q}=-\vec{p}_5)|^2,$$

where F is a kinematic factor containing essentially the phase space distribution, N is a factor due to spin summation and antisymmetrization, $\Phi(\vec{q}=-\vec{p}_5)$

is the Fourier transform of the overlap integral between the spatial wave functions of the target nucleus and the spectator, and $\vec{p}_5$ is the momentum of the spectator. For the ^{3}H$(p, 2p)[nn]$ and ^{3}H$(p, pd)n$ reactions, N equals 1 and $\frac{3}{2}$, respectively, while for the ^{3}He$(p, 2p)d$, the ^{3}He$(p, 2p)d^*$, and ^{3}He$(p, pd)p$ reactions N equals $\frac{3}{2}$, $\frac{1}{2}$, and $\frac{3}{2}$, respectively. Here $[nn]$ and d^* denote an n-n pair and a p-n pair in a $^1S_0$ state with low energy for the relative motion of the pair of nucleons. In the notation adopted $E_i, m_i, T_i, \vec{p}_i$ $(i = 1$ to $5)$ refer to the laboratory total energy, the rest mass, the laboratory kinetic energy, and three-momentum of the incident proton, the target nucleus, and the observed particles in the elements of solid angle $\Delta\Omega_3$ and $\Delta\Omega_4$, respectively, and the spectator particle. When the spectator consists of two unbound nucleons E_5, m_5, T_5, and $\vec{p}_5$ refer to the center of mass of the pair. The quantity $(d\sigma/d\Omega)^{1-4'}$ is properly the square of an off-energy-shell scattering amplitude for the reaction $1 + 4' \rightarrow 3 + 4$ where $4'$ refers to the struck particle inside the nucleus. The off-energy-shell amplitude, however, is generally approximated by a nearby on-energy-shell value, usually corresponding to the center of mass energy of particles 3 and 4 (the final-state energy prescription).

Comparison of the experimental data for the ^{3}He$(p, 2p)d$ and ^{3}He$(p, pd)p$ reactions with PWIA calculations has led to the following conclusions[2]:

(1) The shape of the theoretical momentum distribution for the ^{3}He$\rightarrow p$-d vertex represented by $|\Phi(\vec{q})|^2$ is sensitive mainly to the asymptotic form of the spatial wave function of ^{3}He. The use of an Irving-Gunn wave function for ^{3}He and Hulthén wave function for the deuteron produces a $\Phi(\vec{q})$ which fits reasonably well the shape of the momentum distribution extracted from experiment.

(2) The PWIA predicts cross sections which are too large; the discrepancy increases as the incident energy decreases. Improvement is obtained when the DWIA is used instead.[5]

Similar conclusions also apply to $(p, 2p)$ and (p, pd) quasifree scattering from ^{3}H, as will be shown below.

II. EXPERIMENTAL PROCEDURE

The experiment was performed with a momentum analyzed proton beam from the University of Manitoba sector focused cyclotron. The incident proton energy was 45.6 ± 0.2 MeV [this gives the ^{3}H$(p, 2p)$-nn reaction the same final-state kinetic energy as the previously measured ^{3}He$(p, 2p)pn$ reaction[2]], while the beam energy spread was approximately 300 keV [full width at half maximum (FWHM)]. The target was tritiated titanium consisting of a layer of Ti 4.0 mg cm^{-2} thick with a diameter of 1.25 cm on a 10 mg cm^{-2} gold foil backing. The tritium content of the titanium was quoted by the supplier as 7.6 ± 0.4 Ci. (A subsequent measurement using precise p-^{3}H elastic scattering differential cross-section data[10] showed that this value was correct within the quoted uncertainty.) A dummy target of exactly the same composition but without the tritium served for background measurements. During data taking, each run with the tritiated target was followed immediately by a run with the dummy target. Two detector telescopes with closely similar geometries and each consisting of a 200 μm thick ΔE surface barrier detector, a 1 mm first E surface barrier detector, a 5 mm lithium drifted silicon detector, and a 500 μm veto surface barrier detector viewed the target. The scattering geometry was defined by two pairs of collimators with rectangular apertures. All collimators were made of tantalum 2.5 mm thick. The aperture dimensions of the solid angle defining collimators (width $\times$ height in mm) were 5.54×10.67. The front collimators served as antiscattering baffles only so that particles scattered from the 25 μm thick Kapton-H foil covering the tritium target containment cell could not reach the two detector telescope. The two pairs of collimators were positioned at 4.44 and 11.63 cm from the scattering chamber center. The angular acceptance corresponded to $\Delta\theta = \pm 1.36°$ and $\Delta\Phi = \pm 2.65°$. For the ^{3}He$(p, 2p)$ and ^{3}He(p, pd) measurements ^{3}He gas of 99.5% purity was used. The ^{3}He gas was contained in a 6.2 cm diameter gas cell covered with 25 μm thick Kapton-H foil. The gas pressures were always chosen to be slightly larger than one atmosphere and were read with a precision mechanical pressure gauge to an accuracy of ± 0.05 psi. The gas cell was flushed regularly to prevent buildup of contaminants. The temperature in the cell was measured using a precision mercury in glass thermometer to an accuracy of $\pm 0.5°$. For these measurements the antiscattering baffles used in the tritium experiment were replaced by collimators with the same aperture as the solid angle defining collimators. The polar angle subtended by each of the double aperture systems as defined by the width at half value of the efficiency function was $\Delta\theta \sim 3.9°$. The efficiency function or gas scattering geometry factor was calculated using a slightly modified version of the expression given by Bar-Avraham and Lee.[11] The cross section of the beam at the scattering chamber center was typically 3 mm wide by 7 mm high. Beam currents on target were typically 20 nA. The incident proton beam was captured in a well-shielded Faraday cup. The beam current was integrated using a standard current indicator

integrator. Two monitor counters with closely similar geometries positioned at equal angles (37.5°) left and right with respect to the incident beam direction coincided with the zero-degree axis of the scattering chamber. Viewing a solid target (titanium or nickel), it was required that the ratio of elastically scattered protons observed by the two monitor-detectors was equal to 1.00 ± 0.02. Slight adjustments in the beam transport parameters were made until this requirement was met. The checks were made at the beginning and end of each data taking run. With standard electronics, a timing resolution within the 35 ns separation of cyclotron beam bursts was obtained, thus allowing the separation of the "real" from the "random" coincidence events. The ΔE and total E signals were stored in an on-line PDP 15/40 computer thereby enabling the $(p, 2p)$, (p, pd), and (p, dp) reactions to be measured simultaneously. To permit large counting rates, pileup rejection was imposed on the ΔE signals for pulses arriving within 4 μs of each other. Particle identification was performed off line. The energy calibration of both energy axes was determined from elastic p-^{1}H scattering. Energy loss corrections were made to account for the finite amount of absorber through which the particles travelled before reaching the detector telescopes. The resulting uncertainty in the energies T_3 and T_4 was ±200 keV. The uncertainty in the absolute cross-section scale is estimated to be less than 10% for the tritium measurements and less than 6% for the ^{3}He measurements, while the relative uncertainties in the cross section are taken to be the combined error due to statistics and background subtraction. The data were stored in 64 × 64 arrays for inspection during data collection. For analysis the data recorded with 1024 × 1024 channel resolution were used.

III. RESULTS AND DISCUSSION

^{3}H $(p,2p)[nn]$

Data for the ^{3}H$(p, 2p)nn$ reaction were obtained for coplanar symmetric angle pairs $\theta_3 = \theta_4 = 25°$, 30°, 35°, 38°, 40°, 42.5°, 47.5°, 50°, 55°, and 60°, as well as for coplanar asymmetric angle pairs θ_3-θ_4 = 26°-48°, 30°-45°, 34°-41.5°. The latter three angle pairs as well as the coplanar symmetric angle pair 38°-38° allow zero spectator momentum (the spectator is an unbound n-n pair with zero energy for their relative motion). Except for the coplanar symmetric angle pairs 50°-50°, 55°-55°, and 60°-60°, all T_4 versus T_3 spectra show a pronounced enchancement near the boundary of the four-body continuum. Moreover, the enhancements peak in the region of minimum momentum of the spectator. This behavior is indicative of a p-p quasifree scattering process with a spectator n-n pair with near zero energy for their relative motion which is denoted by ^{3}H$(p, 2p)$-$[nn]$. It should be noted that the differential phase space distribution equals zero at the boundary of the four-body continuum and increases rapidly with increasing invariant mass M_{56} of the two unobserved particles[9]:

$$\frac{dR_4(\vec{P}, E)}{dE_3 d\Omega_3 dE_4 d\Omega_4} = \frac{p_3 p_4}{4} R_2(0, M_{56}),$$

$$R_2(0, M_{56}) = \frac{\pi}{M_{56}} \frac{\{[M_{56}^2 - (m_5^2 + m_6^2)]^2 - 4m_5^2 m_6^2\}^{1/2}}{2M_{56}}.$$

To obtain the projection onto the E_3 (or T_3) axis one integrates over a range of E_4 (or T_4) values determined by the limits on M_{56} ($m_5 + m_6 \leq M_{56} \leq m_5 + m_6 + \Delta$). In the present experiment $\Delta (= T_{nn})$ was chosen as 1.8 MeV. One obtains:

$$\frac{dR_4(\vec{P}, E)}{dE_3 d\Omega_3 d\Omega_4} = \int_{E_4'}^{E_4''} \frac{p_3 p_4}{4} R_2(0, M_{56}) dE_4.$$

For small Δ this can be approximated by:

$$\frac{dR_4(\vec{P}, E)}{dE_3 d\Omega_3 d\Omega_4} = \frac{dR_3(\vec{P}, E)}{dE_3 d\Omega_3 d\Omega_4} \times \frac{1}{\Delta} \int_{m_5 + m_6}^{m_5 + m_6 + \Delta} (2M_{56}) R_2(0, M_{56}) dM_{56},$$

where $dR_3/(dE_3\, d\Omega_3\, d\Omega_4)$ is the three-body differential phase space distribution for a system of three particles with masses m_3, m_4, and $M_{56} = m_5 + m_6 + \frac{1}{2}\Delta$. Accordingly the analysis of the ^{3}H$(p, 2p)[nn]$ reaction was done in a manner similar to the analysis of a three-body final-state reaction. After background subtraction the band corresponding to $T_{nn} < 1.8$ MeV in each four-body continuum was projected onto the T_3 axis. The projected cross sections $d\sigma/(dT_3 d\Omega_3 d\Omega_4)$ were further corrected for accidental coincidences and losses from pileup rejection. The projected cross sections for the ^{3}H$(p, 2p)[nn]$ reaction at coplanar symmetric angle pairs are shown in Fig. 1. In each spectrum the peak occurs at an energy corresponding to the minimum value of the spectator momentum. At larger angle pairs, i.e., 55°-55° and 60°-60°, a quasifree scattering peak is no longer discernible. The projected cross sections for the ^{3}H$(p, 2p)[nn]$ reaction at the coplanar asymmetric angle pairs exhibit peaks at an energy where the spectator momentum equals zero. Peak cross sections were obtained from these spectra using a Gaussian peak fitting routine. All points

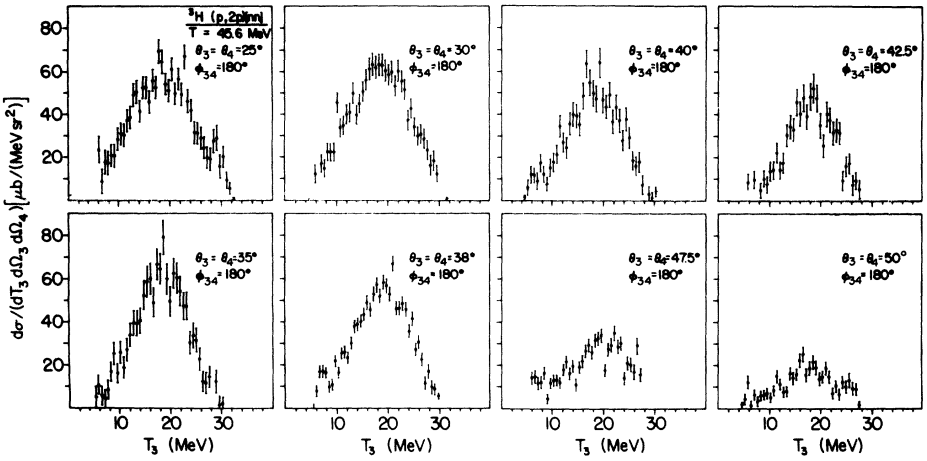

FIG. 1. Energy sharing spectra of the ^{3}H$(p, 2p)$ $[nn]$ reaction at 45.6 MeV and symmetric coplanar angles $\theta_3 = \theta_4 = 25°$, 30°, 35°, 38°, 40°, 42.5°, 47.5°, and 50°.

in the peak to be fitted were weighted by their corresponding statistical error. The peak fitting routine yielded results essentially the same as those obtained when a smooth curve is drawn by eye through the data points around the peak. For the 55°-55° and 60°-60° spectra "peak" cross sections were obtained by averaging the cross section values over a few channels in the region where the spectator momentum is a minimum.

Data for the ^{3}He$(p, 2p)d$ and ^{3}He$(p, 2p)pn$ reactions were obtained at 45.0 MeV for the coplanar symmetric angle pair $\theta_3 = \theta_4 = 38.7°$. The ^{3}He$(p, 2p)d$ events lie near a three-body locus well separated from the four-body continuum. The ^{3}He$(p, 2p)d^*$ events can be identified as a strong enhancement near the boundary of the four-body continuum. Again a restriction was made to relative energies of the unobserved proton-neutron pair $T_{pn} < 1.8$ MeV. Projected cross sections were deduced in a manner similar to the one used for the ^{3}H$(p, 2p)$-$[nn]$ reaction. The spectra in Fig. 2 have shapes similar to one another and also to those of the ^{3}H$(p, 2p)[nn]$ reaction seen in Fig. 1. However, a marked difference exists at the tails of the peaks. Specifically, the ^{3}H$(p, 2p)[nn]$ spectra decrease monotonically at both ends while the ^{3}He$(p, 2p)d^*$ spectrum flattens out at low and high proton energies T_3. The low- and high-energy ends of the energy sharing spectra correspond to low energies for the relative motion of one of the observed protons and the unobserved pair of nucleons which itself has near zero relative energy. The ^{3}He$(p, 2p)d^*$ energy sharing spectra contain a contribution from the $S = \frac{3}{2}$ total spin state for such a p-NN system whereas the ^{3}H$(p, 2p)[nn]$ energy sharing spectra do not. The observed dif-

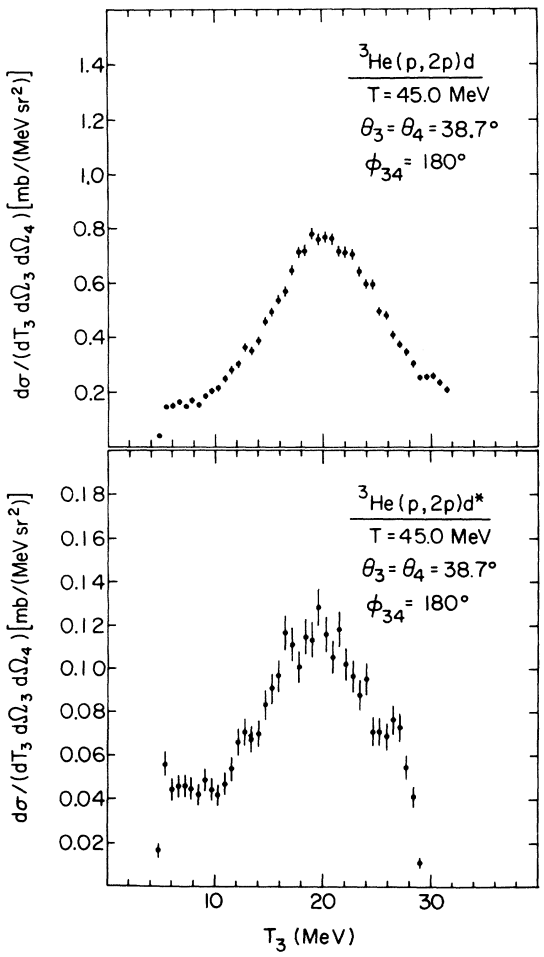

FIG. 2. Energy sharing spectra of the ^{3}He$(p, 2p)d$ and ^{3}He$(p, 2p)d^*$ reactions at 45.0 MeV at the symmetric coplanar angle pair $\theta_3 = \theta_4 = 38.7°$.

ference seems to reflect the well-known fact that low-energy elastic p-d scattering is almost entirely determined by the $S=\frac{3}{2}$ contribution to the cross section.[12] It should further be noted that there exists good agreement between the present data and those obtained previously for the ^{3}He-$(p, 2p)d$ and ^{3}He$(p, 2p)d^*$ reactions.[2] A comparison between the angular correlations for the ^{3}He$(p, 2p)$-d and ^{3}He$(p, 2p)d^*$ reactions and the one for the ^{3}H$(p, 2p)[nn]$ reaction of the present work is shown in Fig. 3. Note the similarities in the shape of the various angular correlations.

The $[nn]$ momentum distribution in ^{3}H was extracted using the PWIA. Figure 4 shows the results obtained using the angular correlation data for four different approximations of the off-energy-shell p-p scattering amplitude. It is evident that there are significant differences in both the shape and magnitude. In particular, the initial-state energy approximation gives results considerably different from those given by the final-state energy approximation. The latter distribution does not peak at $q=0$ but is shifted by ~ 0.05 fm^{-1}. The Stern-Chamberlain and the half-off-energy-shell

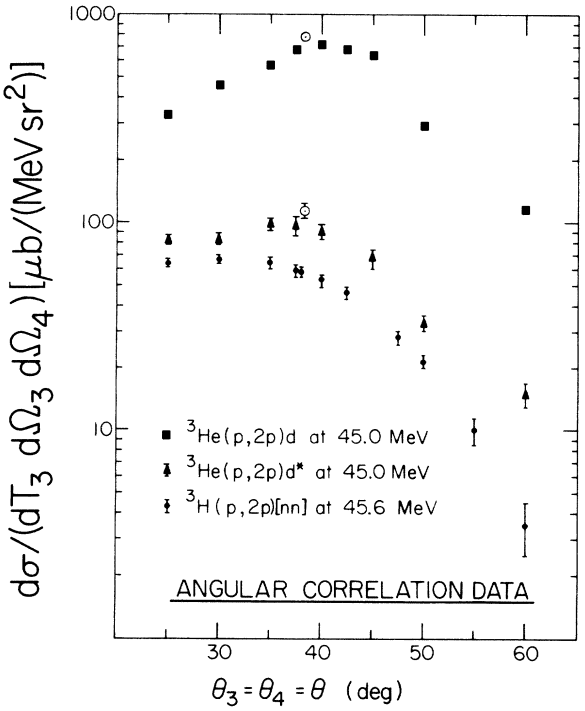

FIG. 3. Comparison of the angular correlation for the ^{3}H$(p, 2p)$ $[nn]$ reaction at 45.6 MeV with those for the ^{3}He$(p, 2p)d$ and ^{3}He$(p, 2p)d^*$ reactions at 45.0 MeV obtained previously (Ref. 2). The data points at 38.7° (open circles) were obtained in the present experiment. They correspond to minimum spectator momentum in the spectra shown in Fig. 2.

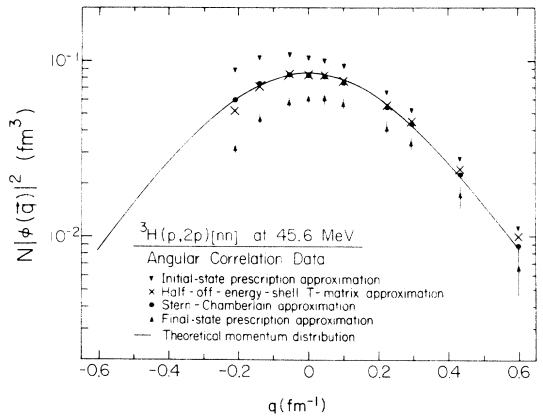

FIG. 4. Momentum distributions for a $p+[nn]$ system in ^{3}H extracted from the ^{3}H$(p, 2p)$ $[nn]$ angular correlation data in the framework of the PWIA and using the initial-state energy approximation, a half-off-energy-shell T-matrix approximation, the Stern-Chamberlain approximation, and the final-state energy approximation to the square of the half-off-energy-shell p-p scattering amplitude. The curve corresponds to a theoretical momentum distribution normalized at peak value to the experimental momentum distribution deduced using the half-off-energy-shell T-matrix approximation. The theoretical momentum distribution was calculated from the overlap of an Irving-Gunn wave function for ^{3}H and a zero energy scattering state wave function for $[nn]$. The Irving-Gunn wave function has a shape parameter $\gamma=1.00$ fm^{-1}.

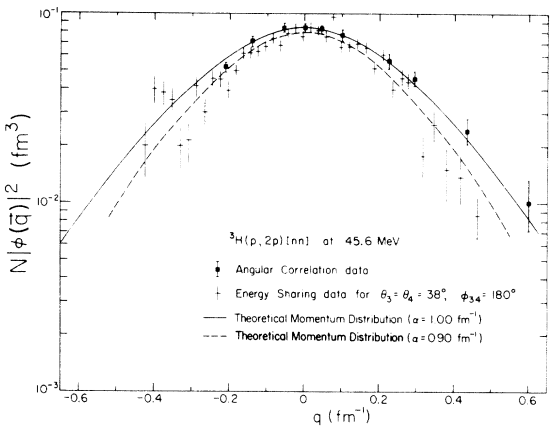

FIG. 5. Comparison between the momentum distributions for a $p+[nn]$ system in ^{3}H extracted from the ^{3}H$(p, 2p)$ $[nn]$ angular correlation and energy sharing data at $\theta_3=\theta_4=38°$ in the framework of the PWIA and using the final-state energy approximation. Also shown is the theoretical momentum distribution of Fig. 5 as well as one calculated with a slightly smaller shape parameter for the Irving-Gunn wave function $\gamma=0.90$ fm^{-1}. The normalizations adopted for the theoretical momentum distributions are somewhat different.

T-matrix approximations[13] produce quite similar momentum distributions which are symmetric about $q = 0$. Note that no error bars are shown except for the final-state energy prescription result. The following convention has been adopted regarding the sign $q = |\vec{q}|$. The quantity q is arbitrarily assigned a positive or negative value whenever the spectator momentum is parallel or antiparallel to the direction of the incident beam or is emitted on the opposite side or the same side as particle 3. The curve represents a theoretical momentum distribution $N|\Phi(\vec{q})|^2$ where $\Phi(\vec{q})$ is the Fourier transform of the overlap integral between an Irving-Gunn wave function for ^{3}H[14] and a zero-energy s-state scattering wave function for $[nn]$.[15] The latter wave function is of the form $\Phi(\rho) = -a_{nn}[1 - \rho/a_{nn} - \exp(\xi\rho)]/\rho$ with $a_{nn} = -16.4$ fm and $\xi = 1.19$ fm.$^{-1}$ The theoretical momentum distribution has been normalized to the data which were extracted using the half-off-energy-shell T-matrix approximation for the p-p scattering amplitude. It is clear that good fits can be obtained to the shapes of the experimental momentum distributions calculated using the Stern-Chamberlain and half-off-energy-shell T-matrix approximations. An equally good fit may also be obtained to the final-state energy approximation results if the theoretical distribution is shifted by ~0.05 fm^{-1} to positive q.

Within the framework of the PWIA, energy sharing data (preferably at an angle pair where zero spectator momentum is kinematically allowed) should give the same momentum distribution as angular correlation data. Analysis of the 38°-38° energy sharing data leads to the following observations: (i) the shapes of the momentum distributions are very similar for all four approximations to the p-p off-energy-shell scattering amplitude; and (ii) the momentum distribution is narrower than the one extracted from the angular correlation data (Fig. 5). Note that exactly the opposite effect was observed for the momentum distributions extracted from the ^{3}He$(p, 2p)$ data[2] reflecting the difference between the low-energy p-nn and p-pn systems. To investigate the angular dependence of p-p quasifree scattering in the ^{3}H$(p, 2p)nn$ reaction measurements were made at the four angle pairs $\theta_3 - \theta_4 = 38°$-$38°$, $34°$-$41.5°$, $30°$-$45°$, and $26°$-$48°$, each allowing zero spectator momentum. The angle pairs chosen correspond to center of mass scattering angles of 90°, 80°, 70°, and 60° for the two outgoing protons. Figure 6 shows the extracted momentum distributions for these angle pairs using the final-state energy approximation. It is evident that each of the momentum distributions peaks at $q = 0$ and has a peak value of approximately 0.055 fm^3. The results indicate that the peak cross section in $(p, 2p)$ quasifree scattering is only a function of the recoil momentum q and not of its direction $\hat{q}$ in the angular range investigated. This is in accordance with what is predicted by the PWIA. However, (p, pn) quasifree scattering studies, of the ^{2}H$(p, pn)p$ reaction[16] for instance, have shown a strong angular dependence of the peak cross section, which is not reproduced by the PWIA predictions. The introduction of attenuation effects on the outgoing nucleons, multiplying the PWIA cross section with a transmission factor, appears to account properly for the observed anisotropy in that particular case.[17]

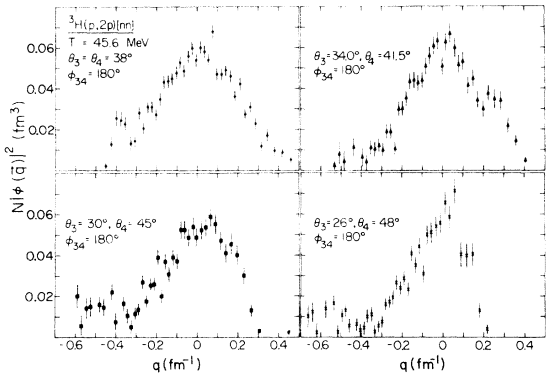

FIG. 6. Momentum distributions for a $p + [nn]$ system in ^{3}H extracted from the ^{3}H$(p, 2p)[nn]$ energy sharing data at $\theta_3 - \theta_4 = 38°$-$38°$, $34°$-$41.5°$, $30°$-$45°$, and $26°$-$48°$ in the framework of the PWIA and using the final-state energy approximation.

^{3}H $(p, 2p)nn$

Spectra for the ^{3}H$(p, 2p)nn$ reaction were formed by projecting the four-body continua after background subtraction onto one of the energy axes (T_3 axis) excluding the band corresponding to 1.8 MeV $> T_{nn} \geq 0$ MeV. The statistically meaningful spectra are shown in Fig. 7. The curves represent phase space predictions, obtained by numerical integration of the four-body differential phase space distributions $dR_4/(dT_3 d\Omega_3 dT_4 d\Omega_4)$.[9] Note that the measured four-body continua had cutoffs defined by $T_3 \lesssim 5$ MeV and $T_4 \lesssim 5$ MeV due to the requirement of the presence of both a ΔE and an E signal from each detector telescope for particle identification. The same normalization was used for all phase space predictions. In general, fair agreement is obtained. However, it can be seen that the spectra for the angle pairs 47.5°-47.5° and 55°-55° show pronounced enhancements over phase space. To understand these apparent enhancements the four-body continua for these two angle pairs are shown in Fig. 8 in a three-dimen-

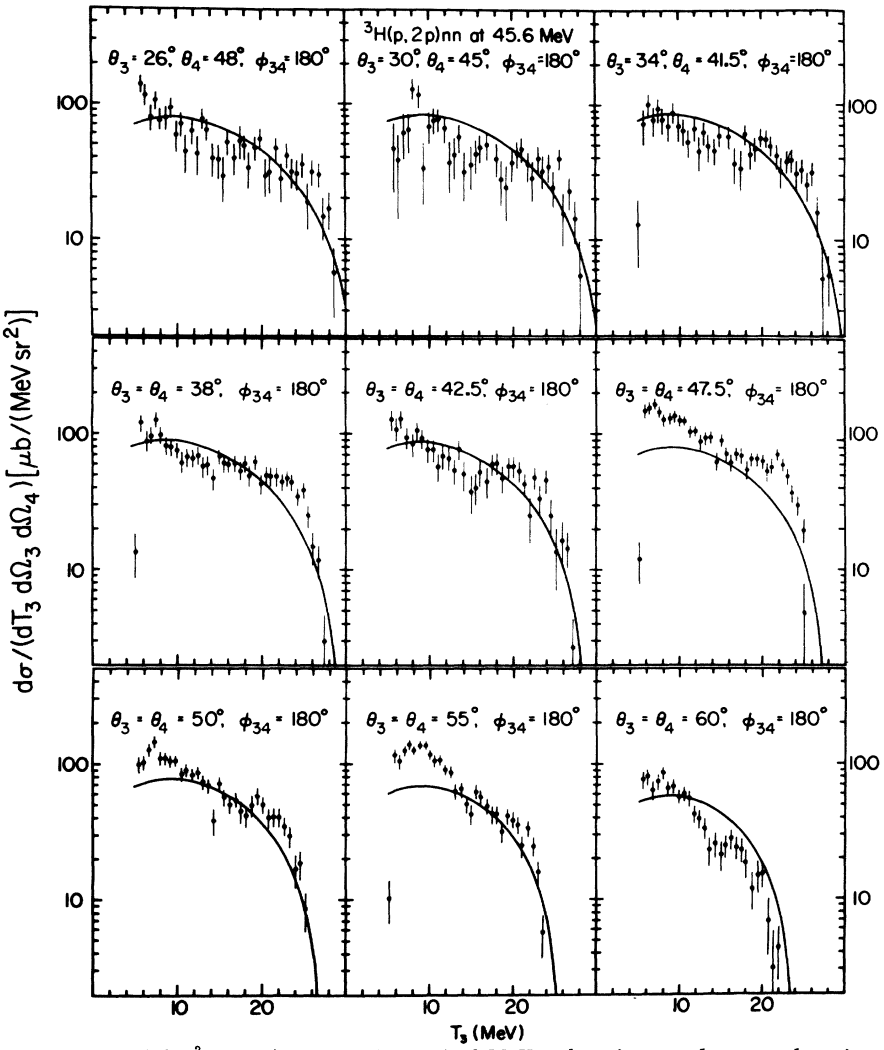

FIG. 7. Projected continua of the ^{3}H(p, 2n) nn reaction at 45.6 MeV and various coplanar angle pairs. The contribution of the ^{3}H(p, 2p) [nn] reaction has been subtracted from the data. The solid curves represent the differential phase space distributions normalized to the experimental results. The normalization factor used is $N_n = 4.96\times10^{-3}$ μb/(MeV^4 sr^2).

sional representation. Arrows indicate where the enhancements in the spectra occur. The enhancements do not appear to be characteristic of a resonant state in ^{3}H. Rather, for the angle pair 47.5°-47.5° the enhancement can be explained in terms of a p-d^* quasifree scattering process where d^* refers to a p-n pair with low energy for their relative motion. The incident proton interacts directly with a correlated p-n pair in the target while the remaining neutron in the target acts as a spectator. The d^* quasiparticle is detected as a proton with half the energy of the d^* system. Some indication for the occurence of a p-d^* quasifree scattering process was also obtained in the previously measured ^{3}He(p, 2p)pn continuum at $\theta_3 - \theta_4 = 50°$-$40°$.[2] For the angle pair 55°-55°, the enhancement can be interpreted as due to a pseudo-two-body process, i.e., $p + t \rightarrow d^* + d^*$ which occurs via neutron pickup. Both d^* quasiparticles are detected as protons with half the energy of the respective d^* systems. Kinematics reproduces the observed positions of the enhancements.

The normalization factor with which the differential phase space distribution $dR_4/(dT_3 d\Omega_3 d\Omega_4)$ have to be multiplied in order to obtain agreement with the projected continua of Fig. 7 is $N_n = 4.96\times10^{-3}$ μb/(MeV^4 sr^2). This should be compared with the corresponding normalization factor for the projected continua of the ^{3}He(p, 2p)pn reaction which has an average value of 13.6×10^{-3} μb/(MeV^4 sr^2).[2] The low-energy cutoff in T_3 and T_4 were approximately the same for both experiments (4.7 and 6.0 MeV, respectively). Thus the four-body cross sections at the ^{3}He(p, 2p)nn reaction are approxi-

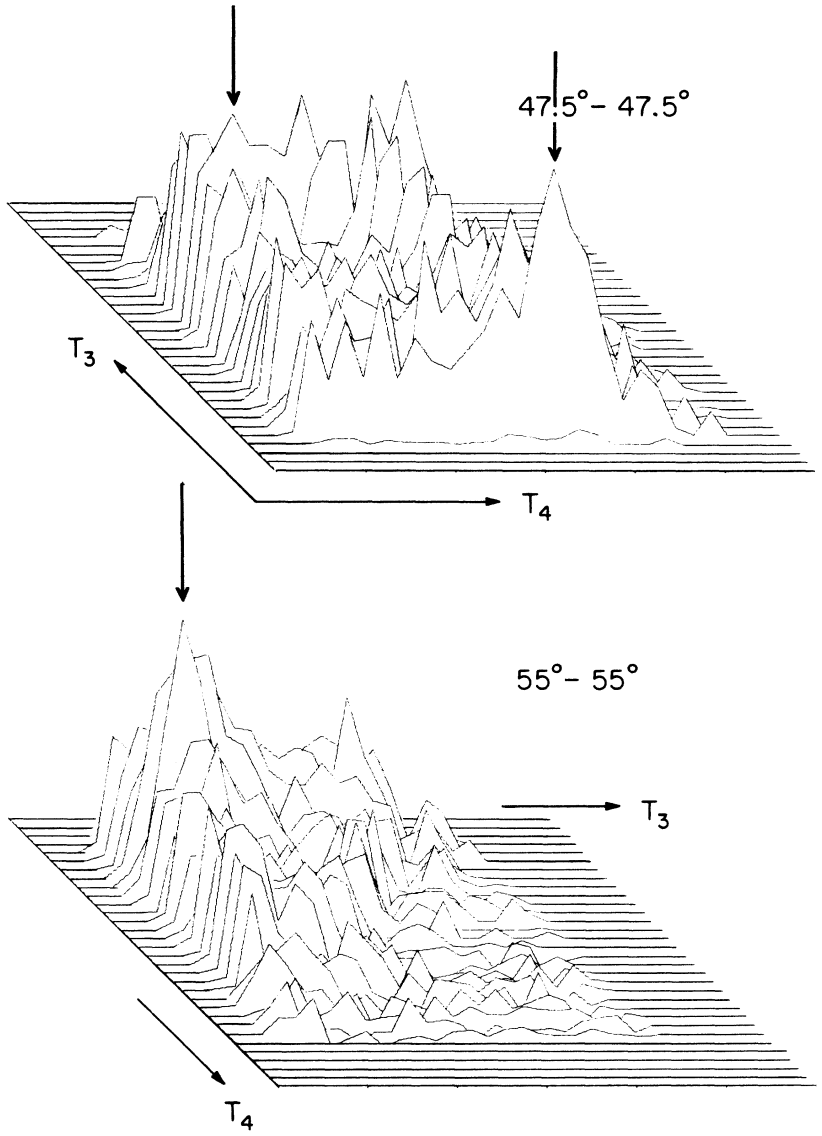

FIG. 8. Three-dimensional representation of the continua of the ^{3}H$(p, 2p)[nn]$ reaction at 45.6 MeV and θ_3-θ_4=47.5°-47.5° and 55°-55°. The vertical arrows indicate enhancements over phase space due to pseudo-two-body processes.

mately 2.5 times as large as those of the ^{3}H$(p, 2p)$-nn reaction. The difference in the continua of the two reactions becomes also quite apparent if presented in the form of invariant mass spectra $d\sigma/(dM_{56}d\Omega_3 d\Omega_4)$ versus M_{56}. Figures 9(a) and 9(b) compare the ^{3}H$(p, 2p)nn$ invariant mass spectrum at 38°-38° with the ^{3}He$(p, 2p)pn$ invariant mass spectrum at 38.7°-38.7°. Note that the ^{3}He$(p, 2p)pn$ spectrum is broader with a smaller ratio of peak to tail cross section, reflecting that both $T = 1$ and $T = 0$ states of the unobserved N-N pair contribute to the cross section.

As corroborated by the analysis of the 20 MeV data[8] it does not appear to be possible to reproduce the invariant mass spectra with a theoretical prediction of the type:

$$d\sigma/(dM_{56}d\Omega_3 d\Omega_4) \sim dR_4/(dM_{56}d\Omega_3 d\Omega_4)(F_s + W_t F_t)$$

unless W_t equals zero. The quantities F_s and F_t are the Watson-Migdal enhancement factors[18] for a $^1S_0$ and $^3S_1$ N-N pair, respectively,

$$F = \frac{1}{k^2 + \left(-\frac{1}{a} + \frac{1}{2} r_0 k^2\right)^2}, \quad (\hbar k)^2 = M_{56} - m_5 - m_6,$$

and W_t is a weighting factor. The curves represent the theoretical predictions for the currently accepted values of the n-n and n-p scattering parameters. Both curves have the experimental energy resolution (Gaussians with 0.60 MeV and 0.50 MeV FWHM) folded in. For the ^{3}He(p, $2p$)pn invariant mass spectrum agreement can only be obtained if it is assumed that the $^3S_1$ contribution can be neglected. Until a more refined theory for four-body reactions is developed, it would seem that a study of reactions such as ^{3}H(p, $2p$)nn and ^{3}He(p, $2p$)pn is not suitable for extracting N-N scattering parameters with any accuracy.

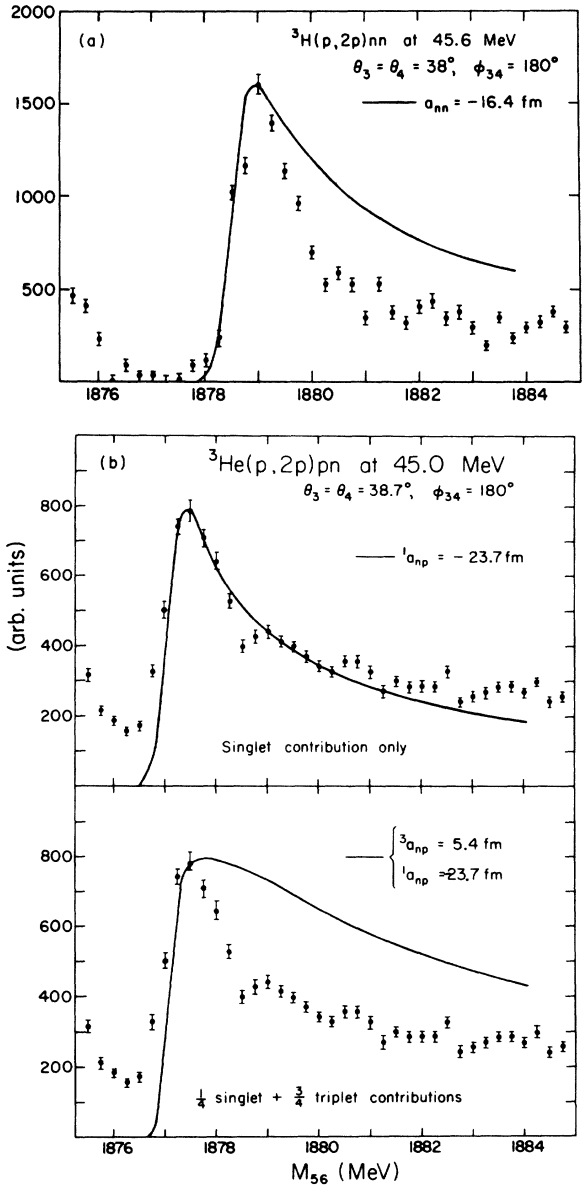

FIG. 9. (a) Invariant mass spectrum of the ^{3}H(p, $2p$)-nn reaction at 45.6 MeV and $\theta_3 = \theta_4 = 38°$. The curve corresponds to the phase space distribution multiplied by a Watson-Migdal enhancement factor (with $a_{nn} = -16.4$ fm and $r_{nn} = 2.7$ fm) and normalized to the experimental peak value. (b) Invariant mass spectrum of the ^{3}He-(p, $2p$)pn reaction at 45.0 MeV and $\theta_3 = \theta_4 = 38.7°$. The curve corresponds to the phase space distribution multiplied by a Watson-Migdal enhancement factor assuming only singlet pn contributions and both singlet and triplet pn contributions, respectively. The curves are normalized to the experimental peak value.

^{3}H (p,pd) n

Data for the ^{3}H(p, pd)n reaction were obtained for coplanar symmetric angle pairs $\theta_3 = \theta_4 = 25°$, 30°, 47.5°, and 55° as well as for coplanar asym-

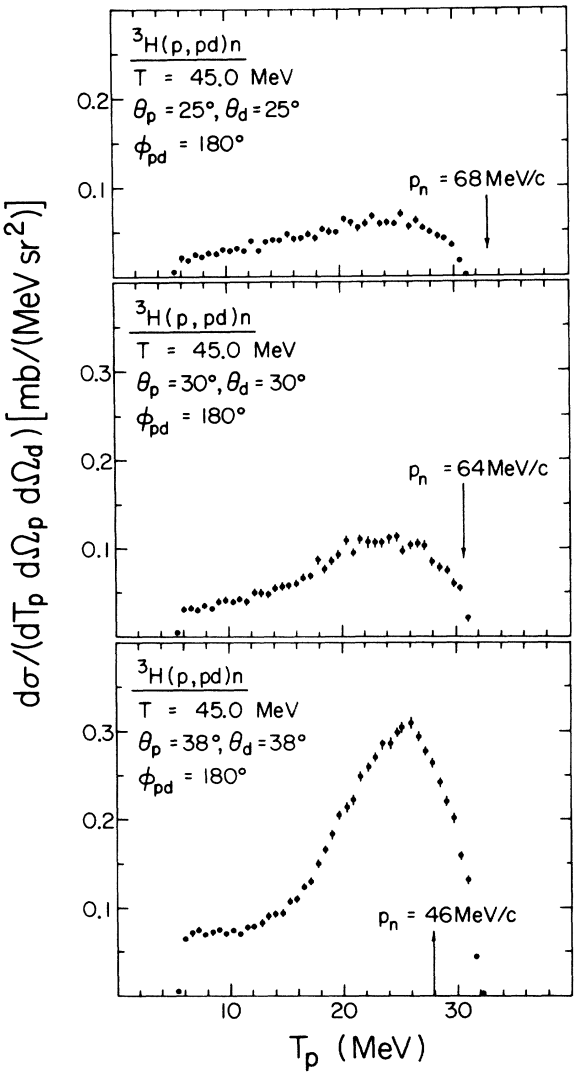

FIG. 10. Energy sharing spectra of the ^{3}H(p, pd)n reaction at 45.6 MeV and symmetric coplanar angles $\theta_p = \theta_d = 25°$, 30°, and 38°.

metric angle pairs 26°-48°, 30°-45°, 34°-41.5°, and 60°-41.6°. The angle pairs $\theta_3 - \theta_4 = 47.5°$-47.5° and 60°-41.6° allow near zero momentum of the spectator. Projected cross sections [onto the proton energy axis (T_3) because of the smaller energy loss corrections required] are shown in Figs. 10 and 11. The arrows indicate the proton energy corresponding to the minimum value of the spectator momentum $p_5 = p_n$ in each spectrum. Except for the spectra at the angle pairs which allow near zero momentum of the spectator, the enhancements do not peak at the position where p_5 is a minimum. Similar shifts in the peak positions have previously been observed for the ^{3}He$(p, pd)p$ reaction at 35 MeV[1] and at 45 MeV.[2] The shifts in the peak positions were interpreted as resulting from a coherent contribution of the amplitude corresponding to a neutron pickup process[19] with an N-N final-state interaction for the remaining nucleons. The peaks appearing on the extreme right of some of the spectra (e.g. at 48°-26°) are a kinematic effect giving an increase in the differential phase space distribution. The 60°-41.6° spectrum shows that the presence of a final-state interaction enhancement significantly alters the shape of the quasifree scattering peak. One should also note that the ^{3}H$(p, pd)n$ cross sections are appreciably smaller than those of the ^{3}He$(p, pd)p$ reaction at the same incident energy.[2]

The effects of the shifts in the ^{3}He$(p, pd)p$ quasi-free scattering peaks are quantitatively demonstrated in Fig. 12, which shows the momentum distributions extracted from the energy sharing data which do not allow near zero spectator momentum. For clarity only representative points from each energy sharing spectrum are plotted. The square of the half-off-energy-shell p-d differential cross section at the final state p-d center of mass (c.m.) energy and the appropriate c.m. scattering angle. The values for $(d\sigma/d\Omega)^{p-d}$ were obtained by interpolation from published cross sections.[20] Although the extracted momentum distributions are not complete, it is apparent that after renormalization to a given value at a certain q, there are differences in both the widths of the distributions and in the shifts from zero spectator momentum.

The momentum distributions extracted from the energy sharing data which allow near zero spectator momentum are shown in Fig. 13. It is apparent that the shape of the extracted momentum distribution from the energy sharing data at 60°-41.6° is appreciably distorted due to the presence of a p-n final-state interaction at $q = -0.6$ fm^{-1}. The only angle pair which seems to be free from competing processes is 47.5°-47.5°, although there is still a slight shift (~ -0.03 fm$^{-1} = 6$ MeV/c) in the peak position. A similar shift has also been observed for the ^{3}He$(p, pd)p$ reaction at 45 MeV[2] and at 65 MeV.[4] At the angle pair 62.8°-41.8° this shift amounts to $\cong -20$ MeV/c at 65 MeV. In the present experiment the shift in the momentum distribution extracted from the 60°-41.6° ^{3}H$(p, pd)n$ data is ~ -0.04 fm$^{-1} = -8$ MeV/c.

A theoretical momentum distribution was calculated as the Fourier transform of the overlap in-

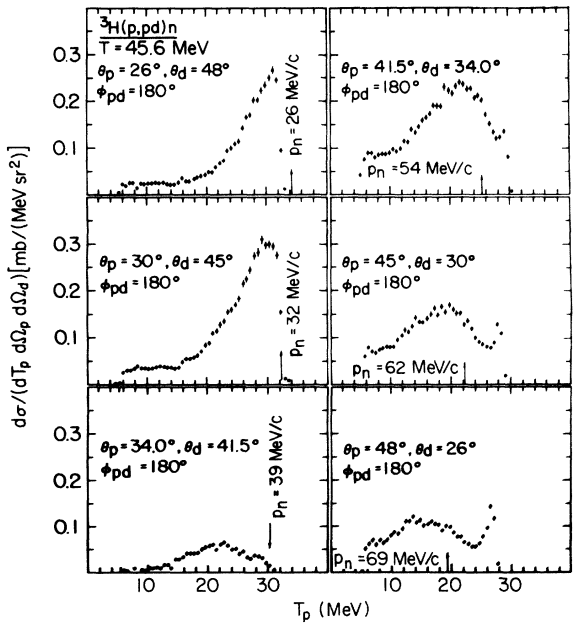

FIG. 11. Energy sharing spectra of the ^{3}H$(p, pd)n$ reaction at 45.6 MeV and asymmetric coplanar angles θ_p-θ_d = 26°-48°, 30°-45°, 34°-41.5°, 41.5°-34°, 45°-30°, and 48°-26°.

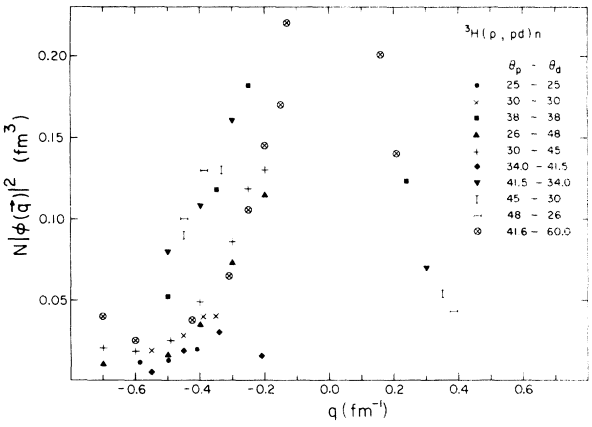

FIG. 12. Momentum distributions for a $p + d$ system in ^{3}H extracted from the ^{3}H$(p, pd)n$ energy sharing data in the framework of the PWIA and using the final-state energy approximation. Only representative points from each of the spectra are shown.

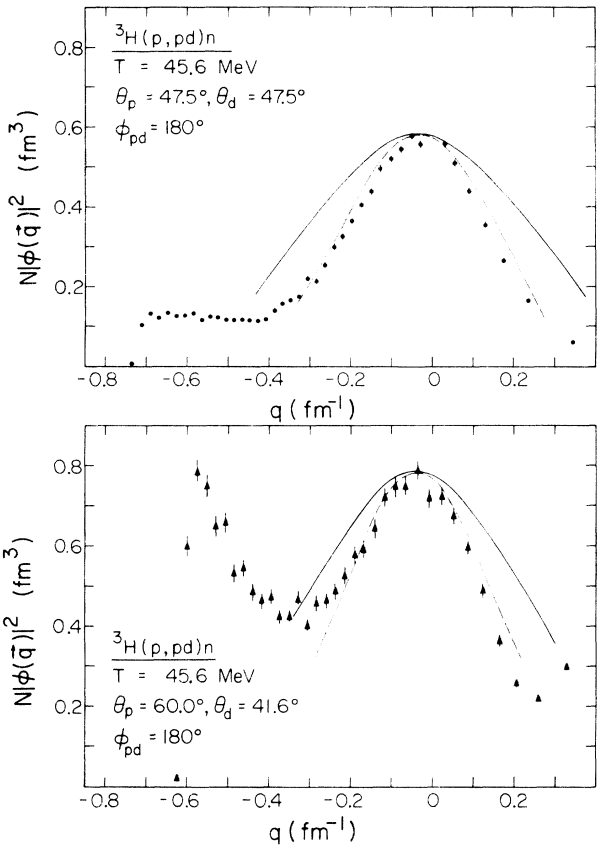

FIG. 13. Momentum distributions for a $p+d$ system in ^{3}H extracted from the ^{3}H$(p, pd)n$ energy sharing data at $\theta_p - \theta_d$ = 47.5°-47.5° and 60°-41.6° (which allow near zero spectator momentum) in the framework of the PWIA and using the final-state energy approximation. The solid and dashed curves correspond to theoretical momentum distributions shifted by −0.03 and −0.04 fm^{-1}, respectively, and normalized at peak value to the experimental momentum distributions. The theoretical momentum distributions were calculated from the overlap of an Irving-Gunn wave function for ^{3}H and a Hulthén wave function for the deuteron.

tegral of an Irving-Gunn wave function for ^{3}H [14] and a Hulthén wave function for the deuteron.[21] From a comparison with the momentum distribution extracted from the 47.5°-47.5° energy sharing data it is obvious that the theoretical $N|\Phi(\vec{q})|^2$ distribution is appreciably wider [64 ± 3 MeV/c half width at half maximum (HWHM)] than the experimental one. Moreover the experimental $N|\Phi(\vec{q})|^2$ distribution is smaller in magnitude. The normalization constant with which the PWIA cross sections (after shifting by −6 MeV/c) have to be multiplied to obtain agreement with experiment at its peak value is $N_n = 0.236 \pm 0.024$. The introduction of a cutoff radius of 4 fm is needed in order to be able to fit the shape of the experimental $N|\Phi(q)|^2$ distribution (43 ± 3 MeV/c HWHM). In this case the normalization constant becomes N_n = 1.35 ± 0.14.

^{3}He$(p, 2p)$, ^{3}He$(p, 2p)d^*$

The analysis of the ^{3}He$(p, 2p)d$ and ^{3}He$(p, 2p)a^*$ energy sharing data at 38.7°-38.7° confirms the results obtained in the earlier experiments.[2]

IV. CONCLUSIONS

In summary, comparing all the data, the following conclusions could be reached:

(i) The shapes of the momentum distributions extracted from the energy sharing data, which allow zero spectator momentum, are very similar for the ^{3}He$(p, 2p)d$ and ^{3}H$(p, pd)n$ reactions (HWHM = 48 ± 3 MeV/c and 43 ± 3 MeV/c, respectively), but those for the ^{3}He$(p, 2p)d^*$ and ^{3}H$(p, 2p)[nn]$ reactions appear to be wider (HWHM = 53 ± 3 MeV/c). However, it should be noted that at many other pairs of angles the energy sharing spectra of the ^{3}H$(p, pd)n$ reaction like those of the ^{3}He$(p, pd)p$ reaction are distorted as a consequence of a strong contribution from the neutron pickup reaction.

(ii) There exist differences between the momentum distributions extracted from angular correlation and energy sharing data [for the ^{3}He$(p, 2p)d$ and ^{3}H$(p, 2p)[nn]$ reactions] pointing out the necessity of further studies at higher proton energies.

(iii) Theoretical momentum distributions derived from the overlap of an Irving-Gunn wave function for ^{3}H or ^{3}He with a two-nucleon wave function fit the shape of the experimental distributions for the ^{3}He$(p, 2p)d^*$ and ^{3}H$(p, 2p)[nn]$ reactions but are too wide for those of the ^{3}H$(p, 2p)d$ and ^{3}H$(p, pd)n$ reactions.

(iv) The PWIA predictions at 45 MeV overestimate the experimental cross sections by a considerable factor.

(v) The four-body continua are reasonably well reproduced by four-body differential phase space predictions except for enhancements due to pseudo-two-body processes.

The authors would like to thank Mark Sybe de Jong for help in data taking and data analysis.

†Work supported in part by the Atomic Energy Control Board of Canada.

*Present address: Department of Physics, University of Riyadh, Riyadh, Saudi Arabia.
‡Present address: Foster Radiation Laboratory, McGill University, Montreal, Quebec H3C 3G1.
§Present address: Nuclear Research Center, University of Alberta, Edmonton, Alberta T6G 2J1.
‖Present address: Power Projects, Atomic Energy of Canada Limited, Mississauga, Ontario L5K 1B2.

[1]I. Šlaus, M. B. Epstein, G. Paić, J. R. Richardson, D. L. Shannon, J. W. Verba, H. H. Forster, C. C. Kim, D. Y. Park, and L. C. Welch, Phys. Rev. Lett. 27, 751 (1971).
[2]M. Jain, S. N. Bunker, C. A. Miller, J. M. Nelson, and W. T. H. van Oers, Lett. Nuovo Cimento 8, 844 (1973); S. N. Bunker, M. Jain, C. A. Miller, J. M. Nelson, and W. T. H. van Oers (unpublished).
[3]H. G. Pugh, P. G. Roos, A. A. Cowley, V. K. C. Cheng, and R. Woody, III, Phys. Lett. 46B, 192 (1973).
[4]A. A. Cowley, P. G. Roos, H. G. Pugh, V. K. C. Cheng, and R. Woody, III, Nucl. Phys. A220, 429 (1974).
[5]R. Frascaria, V. Comparat, N. Marty, M. Morlet, A. Willis, and N. Willis, Nucl. Phys. A178, 307 (1971).
[6]R. Frascaria, V. Comparat, N. Marty, M. Morlet, and A. Willis, in *Few Particle Problems in the Nuclear Interaction*, edited by I. Šlaus, S. A. Moszkowski, R. P. Haddock, and W. T. H. van Oers (North-Holland, Amsterdam, 1972), p. 628.
[7]P. Kitching, G. A. Moss, W. C. Olsen, W. J. Roberts, J. C. Alder, W. Dollhopf, W. J. Kossler, C. F. Perdrisat, D. R. Lehman, and J. R. Priest, Phys. Rev. C 6, 769 (1972).
[8]M. J. Fritts and P. D. Parker, Nucl. Phys. A198, 109 (1972); H. H. Forster, M. Furić, C. C. Kim, D. Y. Park, M. B. Epstein, J. R. Richardson, I. Šlaus, and J. W. Verba, in *Few Particle Problems in the Nuclear Interaction*, edited by I. Šlaus, S. A. Moszkowski, R. P. Haddock, and W. T. H. van Oers (North-Holland, Amsterdam, 1972), p. 624.
[9]W. T. H. van Oers, M. Jain, and S. N. Bunker, Nucl. Instrum. Methods 112, 405 (1973).
[10]J. D. Detch, Jr., R. L. Hutson, N. Jarmie, and J. H. Jett. Phys. Rev. C 4, 52 (1971).
[11]E. Bar-Avraham and L. C. Lee, Nucl. Instrum. Methods 64, 141 (1968).
[12]W. T. H. van Oers and K. W. Brockman, Jr., Nucl. Phys. A92, 561 (1967).
[13]E. S. Y. Tin, Ph.D. thesis, University of Manitoba, 1974 (unpublished).
[14]J. C. Gunn and J. Irving, Philos. Mag. 42, 1353 (1951).
[15]L. Hulthén and M. Sugawara, in *Handbuch der Physik*, edited by S. Flügge (Springer, Berlin, 1957), Vol. 39, p. 106.
[16]V. K. C. Cheng and P. G. Roos, Nucl. Phys. A225, 397 (1974).
[17]R. D. Haracz and T. K. Lim, Phys. Rev. C 11, 634 (1975).
[18]K. M. Watson, Phys. Rev. 68, 1163 (1952); A. B. Migdal, Zh. Eksp. Teor. Fiz. 28, 3 (1955) [Sov. Phys.—JETP 1, (1955)].
[19]M. B. Epstein, I. Šlaus, D. L. Shannon, J. R. Richardson, J. W. Verba, H. H. Forster, C. C. Kim, and D. Y. Park, Phys. Lett. 36B, 305 (1972).
[20]J. D. Seagrave, in *Three Body Problem in Nuclear and Particle Physics*, edited by J. S. C. McKee and P. M. Rolph (North-Holland, Amsterdam, 1970), p. 41.
[21]M. J. Moravscik, Nucl. Phys. 7, 113 (1958).